Size Dependence of Excitons in Silicon Nanocrystals

Nicola A. Hill and K. Birgitta Whaley

Department of Chemistry, University of California, Berkeley, California 94720

Two-particle calculations, which include the electron-hole Coulomb interaction nonperturbatively, are performed for excitons in surface passivated Si nanocrystals. The calculated exciton energies agree quantitatively with photoluminescence data. The exciton charge distributions differ markedly from those obtained in single-particle calculations. The two-particle calculations are compared with single-particle calculations which treat the Coulomb interaction perturbatively. The range of validity for the perturbative treatment of the Coulomb interaction is determined.

Nanometer-sized Si structures photoluminesce efficiently at infrared and visible wavelengths [1]. This observation has prompted many theoretical and experimental studies, both exploring technological applications and investigating the fundamental physical and electronic properties. Porous Si has received particular attention because of its potential use as an optoelectronic material, but the mechanism for its photoluminescence remains a subject of debate. Recently, the dependence of electronic properties on spatial confinement has been determined using a well-defined system of size-selected, surface passivated, Si nanocrystals [2]. The measured photoluminescence energy increases as the nanocrystal size decreases, with peak visible light emission coming from crystallites smaller than 15 Å in diameter. In order to explain the observations, recent publications have called for reliable calculations of the Coulomb interaction between electrons and holes localized on Si particles [3]. In this paper we present the first excited state electron-hole pair calculations for Si nanocrystals, which include the Coulomb interaction nonperturbatively. Using the time-dependent checkerboard propagation technique within a nearest-neighbor tight-binding model [4,5], we perform full two-particle calculations [6] for the nanocrystal exciton. We obtain excellent agreement between our calculated exciton energies and the experimental photoluminescence energies for the entire range of nanocrystals up to 100 Å diam. We calculate the exciton charge distributions and compare them to the charge distributions obtained from single-particle band edge eigenfunctions. The confinement induced mixing of band edge k states is analyzed.

The Si nanocrystals are modeled by adding concentric shells of atoms around a central atom, and saturating the surface dangling orbitals with hydrogen atoms. Ground state properties are determined by evaluating the time evolution of a single-particle electronic wave function, Ψ, using the time-dependent Schrödinger equation, $\Psi(t) = e^{-i\mathcal{H}t/\hbar}\Psi(0)$, with a tight-binding Hamiltonian [4,5]:

$$\mathcal{H} = \sum_i E_i c_i^\dagger c_i + \sum_{j<k} T_{jk}(c_j^\dagger c_k + c_k^\dagger c_j). \quad (1)$$

$c_i^\dagger$ and c_i are the creation and annihilation operators for an electron on site i, and E_i and T_{jk} are the tight-binding parameters, taken from Ref. [7]. An expanded basis of five orbitals ($3s$, $3p_x$, $3p_y$, $3p_z$, and $4s$) on each atom ensures an accurate conduction band edge. Extended Hückel parameters between Si and H atoms are used to simulate the H atoms bonded to the nanocrystal surface [8]. The solution of the time-dependent Schrödinger equation involves making a checkerboard decomposition of the tetrahedral lattice, and propagating the electronic wave function along each of the four bond directions. Eigenfunctions and local densities of states are obtained by Fourier transformation of the wave function time series and the autocorrelation function, respectively.

Excited state properties are determined by calculating the time evolution of a two-particle electron-hole wave function. The standard two-particle tight-binding Hamiltonian is obtained by adding the electron-hole Coulomb interaction to tight-binding terms of the form of Eq. (1), but with the electron and hole restricted to the conduction and valence bands, respectively. The same results are obtained by propagating using the following Hamiltonian:

$$\mathcal{H} = \sum_i E_i c_i^\dagger c_i + \sum_i E_i v_i^\dagger v_i$$
$$+ \sum_{j<k} T_{jk}(c_j^\dagger c_k + c_k^\dagger c_j) + \sum_{j<k} T_{jk}(v_j^\dagger v_k + v_k^\dagger v_j)$$
$$+ \sum_{l \leq m} U_{lm} c_l^\dagger c_l v_m^\dagger v_m, \quad (2)$$

with the initial two-particle wave function chosen to restrict the electron to motion within the conduction band and the hole to motion within the valence band [6]. Here $v_i^\dagger$ and v_i are creation and annihilation operators for a hole on site i. The tight-binding parameters for the hole are set equal to those for the electron. The Coulomb integrals between orbitals on the same atom are evaluated directly using Slater orbitals. The Ohno formula [9] is used to approximate Coulomb integrals between orbitals on different atoms, and the integrals are scaled with a distance-dependent dielectric screening [10]. A calculation of the lowest exciton energy and of the two-particle exciton eigenfunction

is analogous to the determination of the single-particle local density of states and the electron eigenfunction [6]. The excited state electron and hole charge distributions are obtained by calculating the expectation values of the density operators $\delta(\mathbf{r} - \mathbf{r}_{electron})$ and $\delta(\mathbf{r} - \mathbf{r}_{hole})$ over the exciton eigenfunction. Full details of the time-dependent tight-binding method and checkerboard time propagation are given in Refs. [4–6].

Figure 1 shows the calculated band edges and resulting band gap for H-terminated Si nanocrystals up to 100 Å in diameter. At each size, the shift in the valence band edge is approximately double the shift in the conduction band edge. The band gap approaches the bulk value of 1.17 eV asymptotically as the size is increased. Our technique allows the study of the entire range of interesting nanocrystal sizes, whereas conventional time-independent techniques are restricted to structures less than around 40 Å in diameter.

In Fig. 2 we compare our calculated exciton energies with measured photoluminescence energies [2] for Si nanocrystals. Good agreement with the experimental data is obtained at all sizes. According to Schuppler et al., the experimental measurement for the 80 Å diam nanocrystal is larger than our predicted value, because the optical efficiency is highest for the smallest particles in their sample, which emit at shorter wavelengths [11]. The experimental luminescence energy could also be affected by a strain in the thick oxide layer covering the large particles. Recent measurements on large H-terminated Si nanocrystals give values which lie on our calculated line [12]. The slight difference between the exciton and photoluminescence energies for the smallest (around 11 Å diam) nanocrystals could be due to surface localized tail states at the band edges causing the photoemission energy to lie systematically below the exciton energy.

For comparison we have also plotted the results of frequently cited calculations which use (i) real space plane-
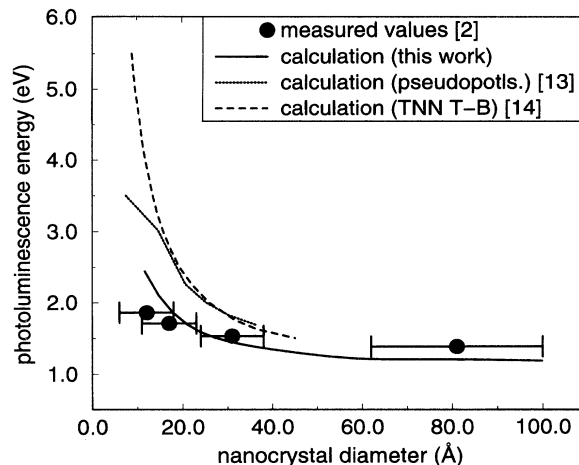
FIG. 2. Comparison for our calculated exciton energies with measured photoluminescence energies for Si nanocrystals [2] and the results of other calculations which use empirical pseudopotentials [13], and third nearest-neighbor tight binding (TNN T-B) with the standard four-orbital basis [14].

wave pseudopotentials [13] and (ii) third nearest-neighbor tight binding with the standard basis of four orbitals per atom [14]. These results were not obtained from full two-particle calculations, but instead the single-particle band gap was calculated, then the contribution of the Coulomb energy was determined using perturbation theory. Both calculations improve over the standard effective mass approximation (EMA) [15], but still predict exciton energies larger than the measured photoluminescence energies by more than 1.5 eV for the smallest nanocrystals studied. The large discrepancy between these results and the experimental observations could be due to either the perturbative treatment of the Coulomb interaction, or to poor prediction of the single-particle band gap. To investigate the source of the discrepancy we have determined the range of validity for the perturbative treatment of the Coulomb interaction by comparing the results of perturbation theory with the results of our full two-particle calculations. We find that the Coulomb energies calculated using the full electron-hole calculation are indistinguishable from the results of perturbation theory and conclude that our improved agreement with experiment is due largely to the accuracy of our tight-binding description with the expanded basis, rather than the nonperturbative Coulomb treatment.

Single-particle band edge eigenfunctions (which ignore the Coulomb interaction) are often used in calculations of optical matrix elements. In order to determine the validity of this simplification, we now compare the electron and hole charge distributions obtained using our full two-particle calculation with the charge distributions in the single-particle band edge eigenfunctions. Figure 3 shows the electron and hole charge distributions in a 147 atom (18 Å diam) Si nanocrystal, obtained using our full two-particle calculation with the Coulomb interaction included. To improve computational efficiency, the sur-
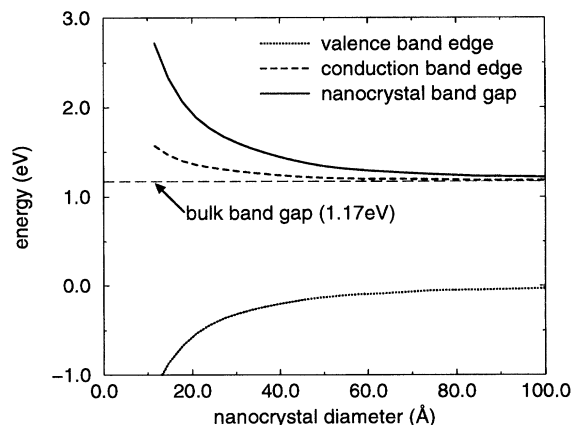

FIG. 1. Calculated band edges and band gaps for Si nanocrystals. The bulk band gap (1.17 eV) is shown for comparison. The band edge positions have an intrinsic uncertainty due to Fourier transformation of a finite time series. In these calculations the uncertainty is ±0.05 eV.
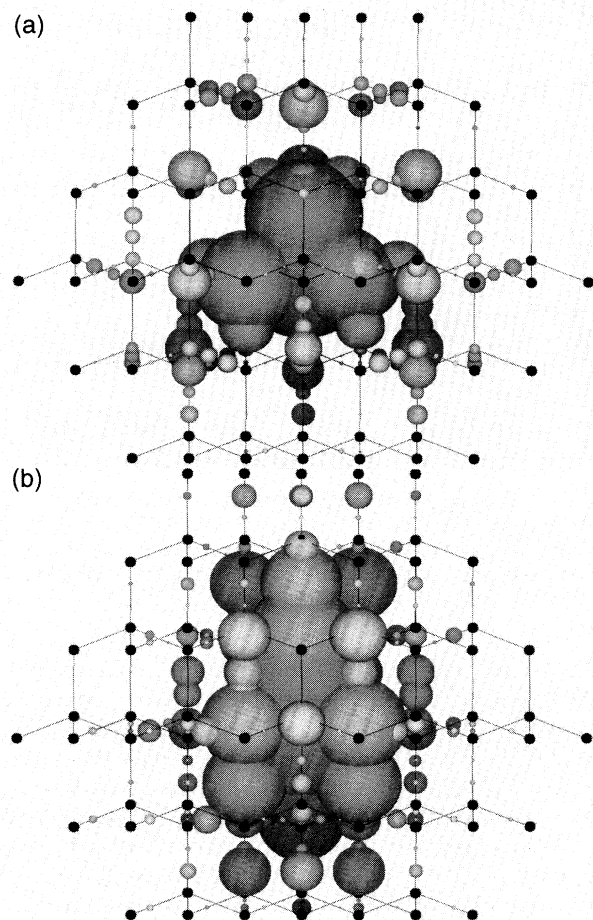
FIG. 3. (a) Electron and (b) hole charge distributions after photoexcitation in a 147 atom (18 Å diam) Si nanocrystal. The Coulomb interaction is included in the Hamiltonian.
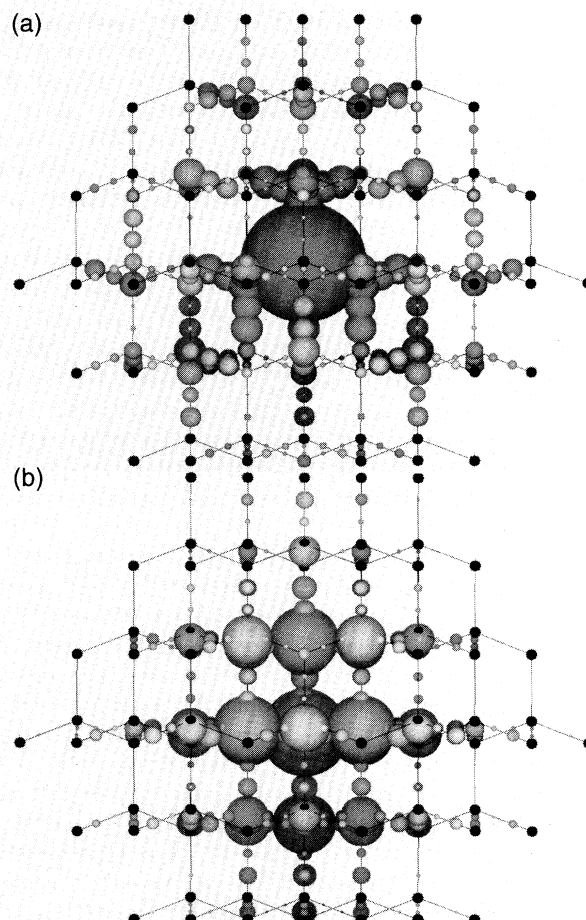

FIG. 4. Probability distributions for the eigenstates at (a) the conduction band edge, and (b) the valence band edge in a 147 atom (18 Å diam) Si nanocrystal. These represent the electron and hole charge distributions after photoexcitation if the Coulomb interaction between the particles is ignored.

face hydrogen atoms and dangling orbitals were not included in the model for the charge density calculations. The small black spheres and black lines show the atoms and bonds, respectively. The gray spheres represent the magnitude of the charge distribution in each sp^3 hybrid or $4s$ orbital. The valence band edge is degenerate, and the Coulomb interaction causes the hole to orient along one of the symmetry axes [Figure 3(b)].

Figure 4 shows the single-particle band edge charge distributions calculated for the same 147 atom Si nanocrystal [16]. Figure 4(a) represents the probability distribution for the electron after photoexcitation if it were not attracted to the hole in the valence band, and Fig. 4(b) represents the probability distribution for the hole if it were not attracted to the excited electron. A comparison with Fig. 3 shows that the attractive Coulomb interaction causes both the electron and hole distributions to shrink towards the middle of the crystallite. The root mean square distance from the center ($r_{rms} = \sqrt{\langle r^2 \rangle}$) for the hole charge distribution decreases from 5.9 Å when the Coulomb interaction is omitted and to 5.2 Å

in the full calculation. Similarly, r_{rms} for the electron decreases from 6.0 to 5.0 Å. The radial changes in the charge distributions are plotted in Fig. 5. The excited state distributions are markedly different from the band edge distributions, suggesting that the band edge eigenfunctions are not good approximations to the true exciton wave functions, and that optical matrix elements for interband transitions must therefore be calculated using full two-particle wave functions with the Coulomb interaction included.

Finally, we project out the k states which contribute to the lowest energy interband transition by Fourier transforming the band edge eigenfunctions of H-terminated nanocrystals. The band edge eigenfunctions in a 100 Å diam nanocrystal correspond to narrow distributions in k space. There is no overlap between the k state distributions for the hole (at Γ) and the electron (near X), and the interband transition is fully indirect. As the nanocrystal size is decreased the electron and hole k distributions broaden by approximately the same amount, until for
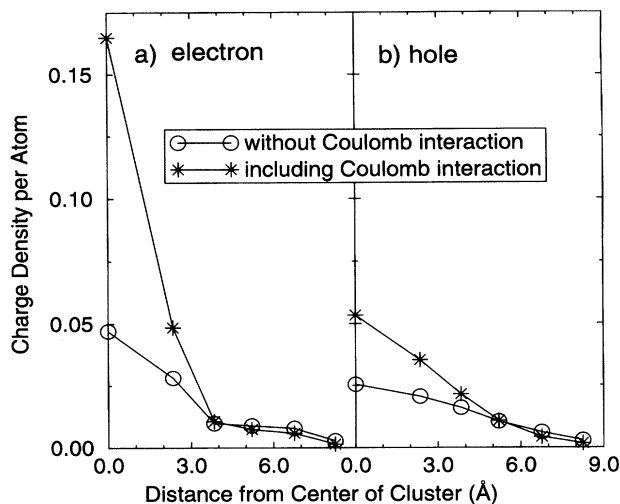
FIG. 5. Radial probability distributions for (a) electron at the bottom of the conduction band, and (b) hole at the top of the valence band, in a 147 atom (18 Å diam) Si nanocrystal. Distributions are shown with and without electron-hole Coulomb interaction.

25 Å diam crystallites the tails of the distributions overlap and a zero phonon radiative transition is weakly allowed [17]. The increasing overlap of the tails is a possible explanation for the observed increase in quantum efficiency with reduced crystallite size [11]. However, even for the smallest nanocrystals studied here (12 Å diam) the peaks of the distributions are at different positions in k space, and the nanocrystals remain primarily indirect gap.

Two separate conclusions can be drawn from the work presented here. First, our calculations have shown that the exciton energies predicted by the time-dependent tight-binding technique agree quantitatively with the measured photoluminescence energies for surface passivated Si nanocrystals up to 100 Å in diameter. Therefore we conclude that the photoluminescence mechanism is dominated by exciton recombination across the gap. The wavelength of the luminescence is determined primarily by the size of the crystallite, which is more important than surface effects in predicting the electronic properties of surface passivated nanostructures. Second, we have determined that the Coulomb interaction may be treated perturbatively in calculating exciton energies for Si nanocrystals without introducing significant error. However, the Coulomb interaction *must* be included when calculating the excited state electron and hole charge distributions (and consequently also the optical properties), because the single-particle band edge eigenfunctions are not good approximations to the exciton wave functions.

In porous Si the surface is unlikely to be fully passivated, and the influence of both surface and size effects on the electronic properties must be considered [18]. Future work will study the effects of surface disorder and reconstruction by calculating two-particle optical absorption spectra for structures with nonideal surfaces using the

time-dependent checkerboard propagation technique. The quantitative agreement with experiment obtained here for surface passivated Si nanocrystals now allows for meaningful studies of both confinement and surface effects in more complex Si structures [19].

[1] L. T. Canham, Appl. Phys. Lett. **57**, 1046 (1990).
[2] S. Schuppler et al., Phys. Rev. Lett. **72**, 2648 (1994).
[3] L. E. Brus et al., J. Am. Chem. Soc. **117**, 2915 (1995).
[4] N. A. Hill and K. B. Whaley, J. Chem. Phys. **99**, 3707 (1993).
[5] N. A. Hill and K. B. Whaley, J. Chem. Phys. **100**, 2831 (1994).
[6] N. A. Hill and K. B. Whaley (to be published).
[7] P. Vogl, H. P. Hjalmarson, and J. D. Dow, J. Phys. Chem. Solids **44**, 365 (1983).
[8] Gaussian Inc., 4415 Fifth Avenue, Pittsburgh, PA 15213.
[9] K. Ohno, Theor. Chim. Acta **2**, 219 (1964).
[10] Z. H. Levine and S. G. Louie, Phys. Rev. B **25**, 6310 (1982).
[11] S. Schuppler et al., Phys. Rev. B (to be published).
[12] V. Petrova-Koch (private communication).
[13] L. W. Wang and A. Zunger, J. Phys. Chem. **98**, 2158 (1994).
[14] C. Delerue, G. Allan, and M. Lannoo, Phys. Rev. B **48**, 11 024 (1993).
[15] T. Takagahara and K. Takeda, Phys. Rev. B **46**, 15 578 (1992).
[16] The calculated electron charge distribution in a H-terminated nanocrystal is less strongly peaked at the center of the cluster than the charge distribution in the truncated nanocrystal shown here. This is because part of the electron density moves onto the bonds with the surface H atoms. In contrast, the hole in a H-terminated nanocrystal is more localized in the interior, since its delocalization onto the surface H atoms is energetically unfavorable [6]. Electron delocalization into the Si-H bonds has also been observed in density functional pseudopotential calculations [T. Uda and M. Hirao, J. Phys. Soc. Jpn. Suppl. B **63**, 97 (1994)].
[17] k-space broadening results from the finite size of the nanocrystal and so is also predicted by simple confinement models based on the effective mass picture. However, detailed EMA calculations show virtually no overlap between the electron and hole envelopes in a 25 Å diameter nanocrystal. [M. S. Hybertson, Phys. Rev. Lett. **72**, 1514 (1994)].
[18] F. Koch, V. Petrova-Koch, and T. Muschik, J. Lumin. **57**, 271 (1993).
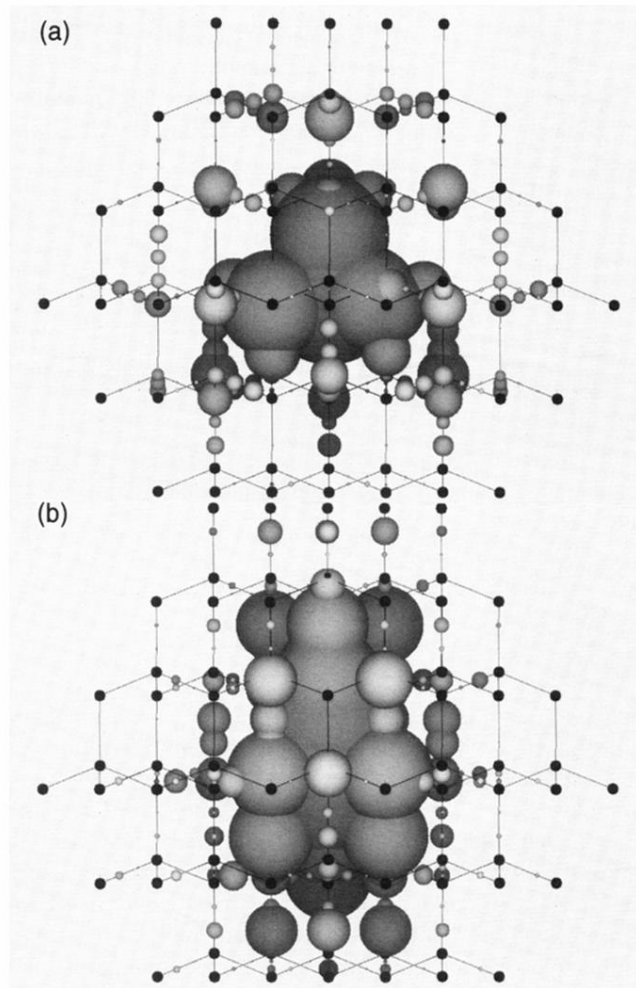[19] N. A. Hill and K. B. Whaley, Appl. Phys. Lett. (to be published).

FIG. 3. (a) Electron and (b) hole charge distributions after photoexcitation in a 147 atom (18 Å diam) Si nanocrystal. The Coulomb interaction is included in the Hamiltonian.
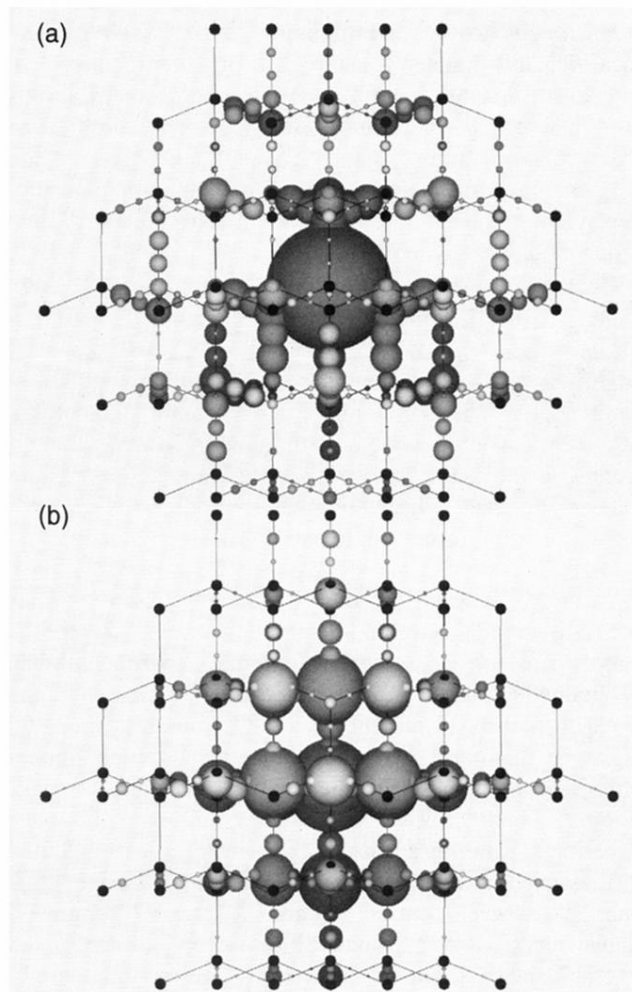
FIG. 4. Probability distributions for the eigenstates at (a) the conduction band edge, and (b) the valence band edge in a 147 atom (18 Å diam) Si nanocrystal. These represent the electron and hole charge distributions after photoexcitation if the Coulomb interaction between the particles is ignored.